



Sono-catalytic degradation and fast mineralization of p-chlorophenol: $\text{La}_{0.7}\text{Sr}_{0.3}\text{MnO}_3$ as a nano-magnetic green catalyst

Samaneh Taherian, Mohammad H. Entezari*, Narjes Ghows

Department of Chemistry, Ferdowsi University of Mashhad, 91775 Mashhad, Iran

ARTICLE INFO

Article history:

Received 22 August 2012

Received in revised form 16 March 2013

Accepted 26 March 2013

Available online 4 April 2013

Keywords:

Perovskite

Nanoparticle

Sonocatalytic degradation

4-Chlorophenol

ABSTRACT

$\text{La}_{0.7}\text{Sr}_{0.3}\text{MnO}_3$ (LSMO) nanoparticles with a perovskite structure were prepared by a combination of ultrasound and co-precipitation method. The synthesized catalyst was characterized by X-ray diffraction, transmission electron microscopy, Fourier transform infrared spectroscopy. The catalytic performance of the catalyst was evaluated for the degradation of 4-chlorophenol in the presence and in the absence of ultrasound. The degradation has been studied at different temperatures, pH, catalyst dosage, and initial concentration of 4-chlorophenol. The results have shown that the degradation efficiency was higher in the presence of ultrasound than its absence under the mild conditions. More than 88% decrease in the concentration and 85% decrease in the TOC for 4-chlorophenol could be achieved in a short time of sonication with respect to the conventional method. This behavior could be attributed to the cavitation process which followed by a high mass transfer on the catalyst with high surface area. These conditions led to facilitate the removal of pollutant from aqueous solution. The results also indicated that the catalyst without recalcination can be used successfully up to five consecutive cycles without any significant loss in activity in the presence and in the absence of ultrasound. In addition, the most important is the magnetic property of the nanoparticles which separated easily from aqueous solution by an external magnetic field.

© 2013 Elsevier B.V. All rights reserved.

1. Introduction

One of the most toxic phenolic compounds is 4-chlorophenol (4-CP) which used in the synthesis of higher chlorinated chemicals, dyes, drugs and pesticides [1]. 4-CP is released into the environment as a byproduct of various industries, including the chlorinated bleaching of paper and chlorination of drinking water, drug decay, and via industrial wastewater discharge. It imposes serious dangers to the environment due to its high toxicity, carcinogenic character, persistence in the environment, and low biodegradability [2]. Hence, great attention has been paid on its removal from the wastewater [3–5].

Available methods to deal with phenolic compounds include activated carbon adsorption, chemical oxidation, biological digestion, photocatalytic degradation, etc. [6–8]. However, these methods have their limitations and disadvantages. In many cases, these methods are not appropriate to use for the removal of low levels of pollutants, or the recovery is not economically feasible in very low concentrations [9]. Therefore, it is necessary to use advanced techniques for the removal of pollutants and their mineralization.

Recently, great attention has been paid to the use of ultrasound as one of the wastewater treatment technologies due to its greater efficiency and easier method to operate [2,10–12]. The chemical effects of ultrasound derive from acoustic cavitation i.e. the formation, growth and implosive collapse of cavitation bubbles in a liquid due to localized extreme conditions [13]. But the total mineralization of organic pollutants by ultrasound irradiation alone, is still a difficult task especially for persistent organic compounds. To improve the degradation efficiency, ultrasound can be used while coupled with other techniques [2,11,14–18]. As a result, a proper combination can increase the degradation and decrease the process time [14–18].

Among different catalysts, little attention has been paid to perovskite materials (ABO_3) for the destruction of organic pollutants such as phenolic compounds [19–22]. They have attracted a great interest due to its environment friendly properties. Sr-doped LaMnO_3 or LSMO is particularly of interest owing to its proper magnetic, electric, catalytic properties, non-toxicity, ease of handling, stability at very high temperatures, high resistance to dissolution in aqueous/organic solvents or acidic and basic media [23], and biomedical applications [24].

Recently, the cytotoxicity of synthesized LSMO nanoparticles has been evaluated. The result has showed that the synthesized nanoparticles were not toxic and this is critically important for real-world applications [24–26]. Great efforts have been made in

* Corresponding author.

E-mail address: moh_entezari@yahoo.com (M.H. Entezari).

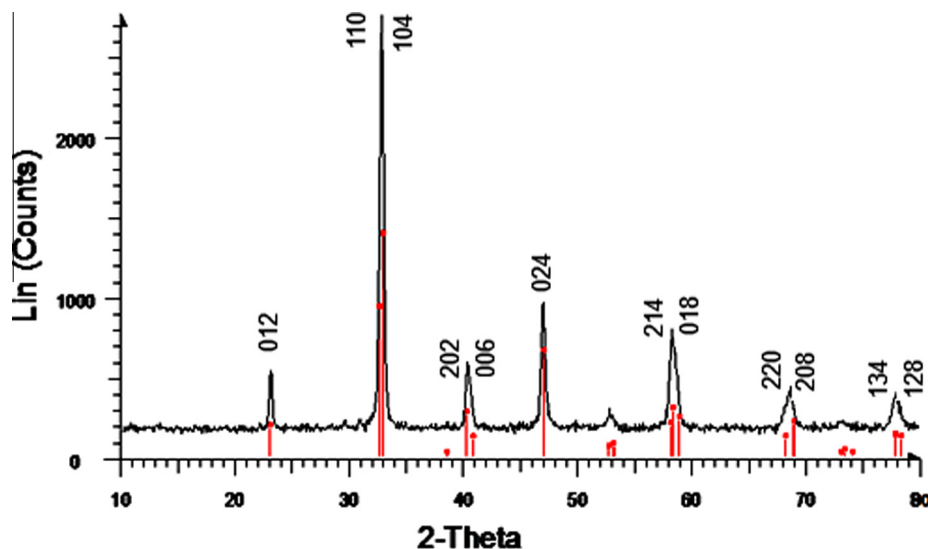


Fig. 1. XRD pattern of the synthesized LSMO.

the field of green chemistry to adopt methods that use less toxic chemicals, less energy, and produce fewer by products [27,28]. Hence, using of combination ultrasound and catalyst (LSMO) for pollutant degradation constitutes a very important direction in green chemistry for environmental applications.

Different methods have been reported to prepare perovskite materials, such as the versatile chemical technique [29], anodized alumina oxide template [30], hydrothermal [31–33], homogeneous co-precipitation [34], ultrasound [35]. Generally, these methods have some disadvantages such as complexity in the procedure [30] and long reaction time [31–33]. But, ultrasound is an easy method to operate under mild conditions [36–42].

To the best of our knowledge, there is no report on the p-chlorophenol degradation by a combination of ultrasound and LSMO nanoparticles. In the present work, LSMO nanoparticles were prepared by ultrasound and co-precipitation. The catalytic activity of LSMO is investigated in p-chlorophenol degradation under ultrasound and classical methods, as well as the optimization of the process. Its reusability was also investigated and found to be quite stable with excellent catalytic activity even after 5 recycles. In addition, easier workup, higher decomposition efficiency, shorter reaction time, decrease of TOC, and magnetically recoverable can be considered as advantageous of this study.

2. Experimental

2.1. Materials

High-purity KMnO_4 , KOH , $\text{MnCl}_2 \cdot 4\text{H}_2\text{O}$, $\text{LaCl}_3 \cdot 6\text{H}_2\text{O}$, and $\text{Sr}(\text{NO}_3)_2$ were used as starting materials. KMnO_4 , $\text{Sr}(\text{NO}_3)_2$ and $\text{LaCl}_3 \cdot 6\text{H}_2\text{O}$ from BDH, KOH , 4-chlorophenol from Riedel, and $\text{MnCl}_2 \cdot 4\text{H}_2\text{O}$ from Merck were used without further purification. The stock solution of 4-chlorophenol was prepared in de-ionized water with concentration of 1000 mg L^{-1} . These solutions were diluted as required to obtain the solution with specific concentration. The required pH adjustment was done using NaOH and HCl solutions.

2.2. Preparation and characterization of the catalyst

LSMO nanoparticles were synthesized by sonication-assisted co-precipitation (Branson Digital sonifier, Model W-450 D, output

acoustic power 40 W, normal horn) with some changes [35]. Stoichiometric amount of $\text{LaCl}_3 \cdot 6\text{H}_2\text{O}$, $\text{Sr}(\text{NO}_3)_2$ and $\text{MnCl}_2 \cdot 4\text{H}_2\text{O}$ dissolved in 75 mL de-ionized distilled water in a beaker (solution A). Then, 25 mL of solution B contains KMnO_4 and KOH , is slowly dropped into solution A under sonication. The solution was continued to sonicate at room temperature for 30 min. During sonication, the temperature of the reaction was raised to ca. 75°C by stopping the circulating bath. The brown suspension was centrifuged and then it was washed with distilled water five times. The product was suspended in ethanol under sonication for 7 min, centrifuged and dried at 100°C for 1 h. The fully crystallized black LSMO nanoparticles with magnetic properties were obtained after calcination in air at 900°C for 1 h.

The prepared samples were characterized by X-ray diffraction (XRD, Bruker-axs, D8 advance model), transmission electron microscopy (Hitachi H8 100 (200 kV) equipped with analyzing system EDAX Link ISIS), and Fourier transform infrared spectroscopy (FTIR, Shimadzu 4300). The zeta potential of the nanoparticles was determined by zetasizer (MALVERN NANO-ZS90).

Fig. 1 shows the XRD pattern of the prepared LSMO nanoparticles. All of the peaks can be identified as the LSMO perovskite phase. It reveals that the XRD peaks in the pattern can be indexed to the (012), (110), (104), (202), (006), (024), (214), (018), (220), (208), (134), (128) planes for the hexagonal structure by Celref software. This pattern indicates that the sample is fully crystallized, and no impurity can be detected by XRD. Particle size was calculated from the X-ray line broadening, using the Debye-Scherrer equation. The average particle size was about 23 nm.

Fig. 2(a, b) shows the TEM of the as-synthesized samples and Fig. 2(c, d) the calcinated samples at 900°C . It is clearly seen from the TEM images that the particle size increases with calcination. Size distribution was also determined as shown by histogram in supporting (Fig. 1S). The particles after calcination at 900°C have a distribution from 25 to 150 nm, with an average diameter of 72 nm. The corresponding selected area electron diffraction patterns in Fig. 2(e, f) show spotty ring patterns, calcination results in stronger spotty pattern, indicating larger particle size with highly crystalline structure.

Fig. 2S(a) in supporting shows the infrared spectra of the synthesized LSMO before calcination. The peaks at 1630 and 3500 cm^{-1} are related to the O–H group. The perovskite oxides with basic properties can absorb CO_2 which is slightly acidic on

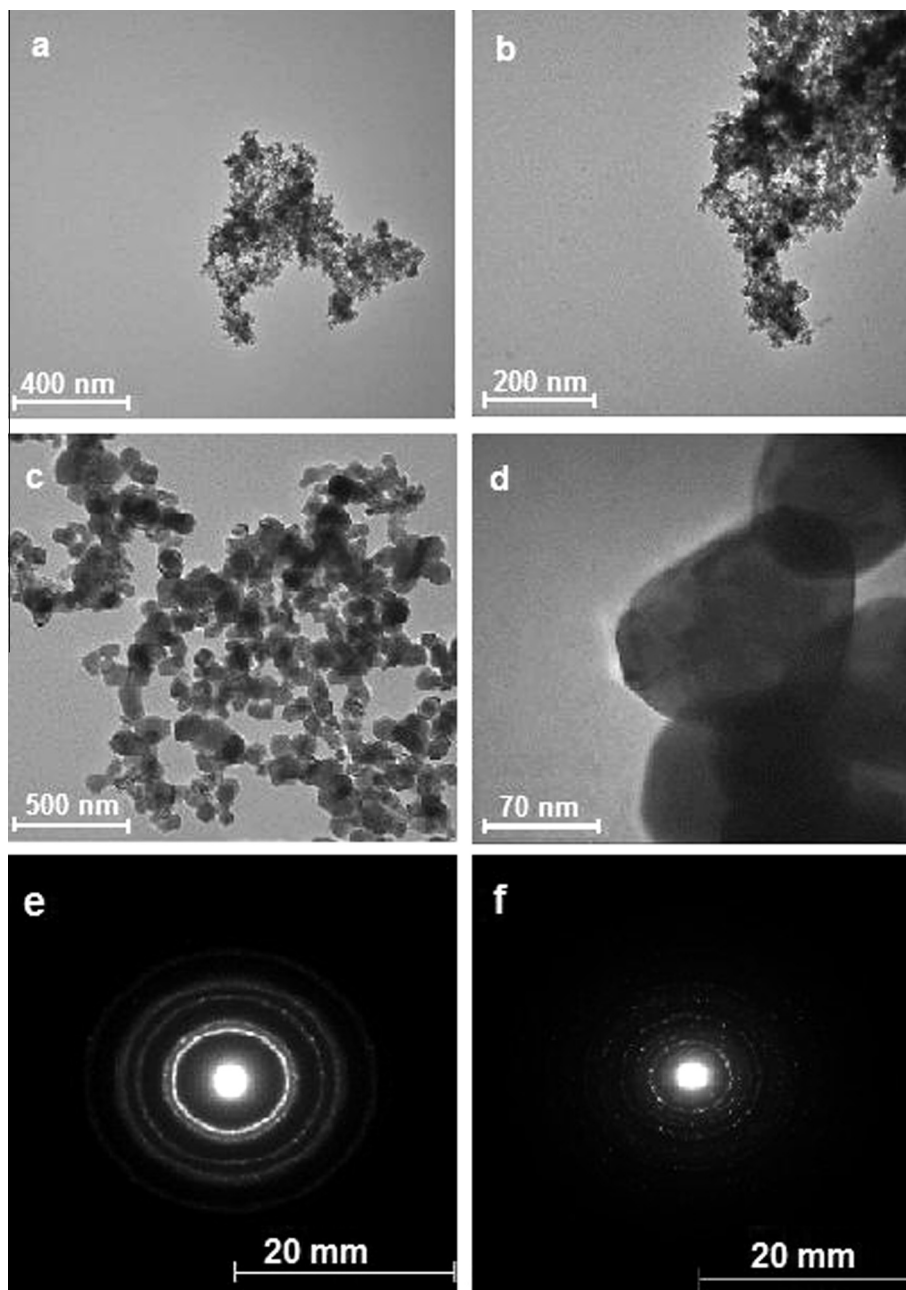


Fig. 2. TEM micrograph of the as-synthesized (a, b) and calcinated (c, d) LSMO samples. SAED patterns of as-synthesized (e) and calcinated sample (f).

the basic sites. Upon CO_2 adsorption on perovskites the monodentate and bidentate carbonates are formed. The peaks in the range of $1362\text{--}1546\text{ cm}^{-1}$ are ascribed to the stretching vibrations of the carbonate groups [43]. In addition, the absorption band at $860\text{--}900\text{ cm}^{-1}$ could be related to the CO_3^{2-} functional group. These bands may correspond to the carbonate impurity phase which disappears after calcination at $900\text{ }^\circ\text{C}$ (Fig. 2S(b)). The main absorption band around 600 cm^{-1} in Fig. 2S(a, b) related to the metal–oxygen bond, indicating the formation of the perovskite. This is due to the change in Mn–O–Mn bond length in MnO_6 octahedral [25].

2.3. Catalytic degradation

The catalytic experiments were carried out in the presence of ultrasound with equipment operating at 20 kHz (Branson Digital sonifier, Model W-450 D, output acoustic power 36 W, normal horn). A total of 50 mL of 4-chlorophenol solution (50 mg/L) con-

taining nanocatalyst (0.07 g) was sonicated for 10 min in a Rosset cell at initial pH of 2.5. The experiments without ultrasound (control method) were performed in a batch reactor with stirring at 400 rpm. The temperature was controlled by a circulating bath at $20\text{ }^\circ\text{C}$ for both methods. Then, the aqueous phase was separated from solid catalyst by Universal 320 centrifuge (Zentrifugen het-tich), and the final concentration of the chlorophenol determined with a UV–vis spectrophotometer (unico 2800) at 280 nm. The pH of the samples was measured using calibrated pH meter (827 pH Lab). The total organic carbon (TOC) of the samples was determined by a TOC-V CSN analyzer (model Shimadzu).

3. Results and discussion

Preliminary experiments were carried out over LSMO sample with the purpose of monitoring the catalytic performance for the

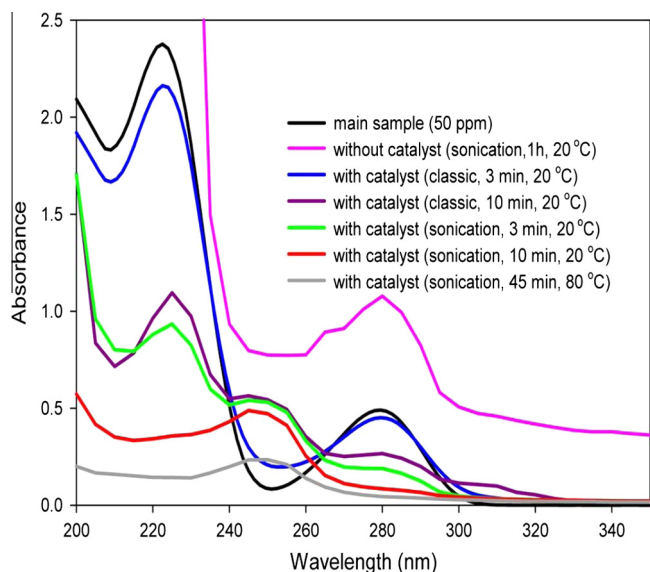


Fig. 3. UV absorption spectra of 4-CP solution at different times at pH = 2.5.

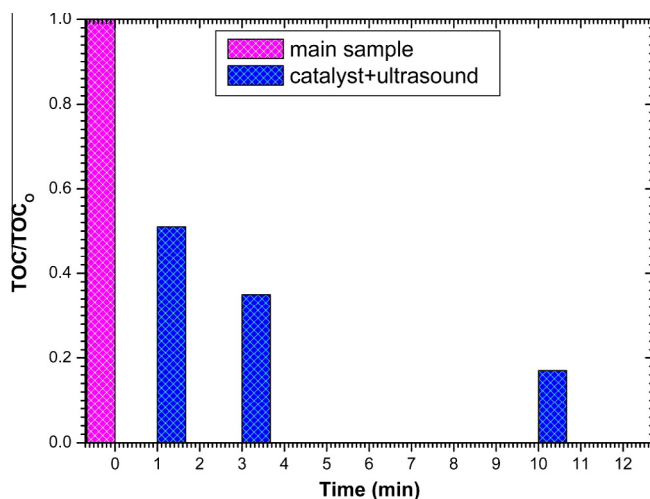


Fig. 4. Changes of TOC with time.

4-CP removal in the presence of ultrasound. These experiments were done with an initial 4-CP concentration of ca. 50 mg L^{-1} and 0.07 g catalyst at $20 \text{ }^\circ\text{C}$. Fig. 3 shows the UV absorption spectral changes during the degradation process. The absorption bands at 225 and 280 nm in the main sample are characteristic of the chlorophenol. The absorption intensity of these bands decreases continuously and a new absorption band develops at $\sim 250 \text{ nm}$. This band has been associated to the formation of cyclic intermediate. But, the concentration of this intermediate is very low and vanishes at longer times. The intermediate might be related to the benzoquinone that has an absorption band at $\sim 248 \text{ nm}$ [44]. The structure of intermediate was confirmed by the UV absorption spectra of benzoquinone solution at different pH (Fig. 3S in supporting).

For considering the fate of degradation, the solid and liquid phases should be checked for the final products of degradation. Fig. 4S in supporting shows the FTIR spectra of LSMO before and after contact with solution containing 4-CP. There is no difference between the two spectra (a and b). This means that 4-CP does not adsorb on the surface and the byproducts cannot be observed on the nanoparticle's surface too.

For checking the aqueous phase, Fig. 4 shows the total organic compound (TOC) of the solution at different interval times. A reduction of 85% of TOC under ultrasound and 58% in conventional method were obtained in 10 min. This reduction confirmed the low concentration of intermediate after treatment of the solution. In addition, the chloride ion formed via the degradation of 4-CP increases with time (Fig. 5S in supporting) which is in agreement with the removal of TOC.

3.1. Optimization of the catalytic degradation

The catalytic degradation of 4-CP over LSMO is optimized in the presence and absence of ultrasound by considering the effect of important variables on the degradation process.

3.1.1. The pH of medium

Fig. 5(a, b) show the absorption spectra of 4-CP in the main samples and in the samples with catalyst at various pH and Fig. 6S in supporting shows the degradation rate versus the pH (ca. 1–10). As it is observed, the absorption spectra of 4-CP (main sample) has been only shifted in alkaline solution and no intermediate was formed in the presence of the catalyst. The maximum degradation efficiency was observed at pH 2.5 with formation of intermediate in the presence of the catalyst. Since the initial and final pH of the solution are acidic, the appeared pick at $\lambda = 250$ is not related to 4-CP (Fig. 3S in supporting).

The pH is the most important factor for the removal of pollutant in this work. The rates of degradation are varied by changing the pH which is related to the specification of pollutant molecule i.e. whether the pollutant is present as ionic species or as a molecule and the surface's charge of the catalyst.

The variations of the degradation rate are attributed to the variable ratio of ionic form to neutral component of 4-CP at different pH based on Henderson equation. The rate of degradation is lowest in alkaline solution. This should be explained by the ratio of anionic form to the molecular form which calculated at different pH. These ratios are 1.99×10^{-7} , 1.99×10^{-6} , 0.025 and 6.309 at pH, 2.5, 3.5, 7.6 and 10, respectively. At pH lower than 2.5, 4-CP can be protonated and due to the high positively charge of the nanoparticles at these pH, the degradation decreased. On the other hand, the z-potential of the nanoparticles was measured and it was changed from nearly +24 mV to +40 mV by changing the pH from 7 to 2.5. Both forms exist at pH = 2.5 and the majority form is neutral. The electrostatic attraction between the high positively charged surface at pH = 2.5 and the anionic form (with very low concentration) of the pollutant in the solution led to the adsorption and shift the equilibrium to the production of anionic form and this process continued to complete removal. In all selected pH, the presence of ultrasound was more effective than conventional method. This should be explained based on adsorption on the surface and the higher mass transfer of organic molecule between the liquid phase and the catalyst surface which are due to the shock-wave and microjet produced by the cavitation process. In addition, the presence of particulate matter can play a critical role in different ways for oxidation of pollutants in water solution irradiated with ultrasound. The presence of dispersed particles in solution during sonication provides additional nucleation sites for cavity formation over its surface, enhancing the number of microbubbles in the solution. Moreover, this fact has been proven to be influenced by the roughness of the particles. Dispersed particles can also act as a wall for the bubbles transmission, producing an asymmetric collapse of the cavitation bubbles and leading to the generation of a large number of tiny bubbles in the liquid solution. Both of them produce an increase of microcavities that enhance the efficiency of the sonochemical oxidation [45–47]. The asymmetric collapse of microbubbles over the solid surface, turbulent flow and

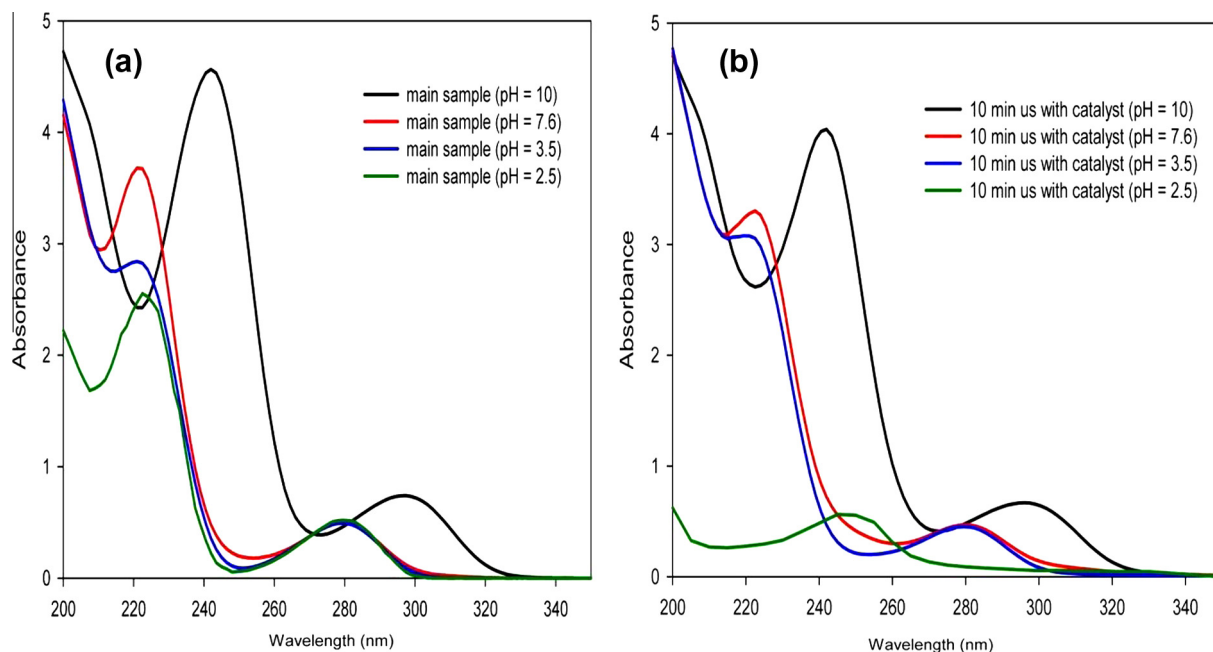


Fig. 5. Effect of pH on the degradation of 4-CP in the main sample (a) and in the presence of the catalyst (b) (stirring speed, 400 rpm; initial concentrations, 50 mg L⁻¹; temperature, 20 °C; time, 10 min; catalyst dosage, 0.07gr).

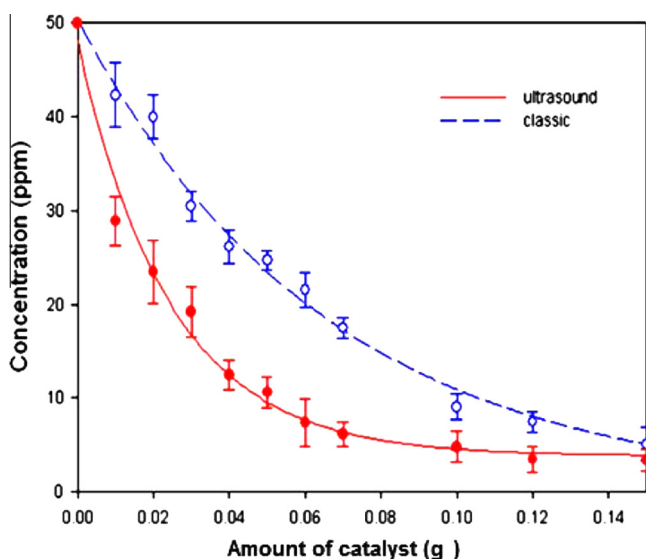


Fig. 6. Effect of the amount of catalyst on the degradation of 4-CP, (concn. 50 mg L⁻¹; temp. 20 °C; time 10 min).

shock waves generated by cavitation in liquids irradiated with ultrasound offered additional degradation of adsorbed pollutant. The result of blank experiment (without catalyst) in the presence of ultrasound should also be confirmed that the particulate matter can play a critical role in the decomposition of the pollutant (Fig. 3).

3.1.2. The amount of catalyst

The degradation of 4-CP on LSMO in the presence and absence of ultrasound was studied by changing the amount of catalyst in aqueous solution while the other variables were kept constant.

Based on Fig. 6, by increasing the mass of catalyst the degradation was increased for both methods which is due to the availability of higher surface area and active sites of the catalyst. The

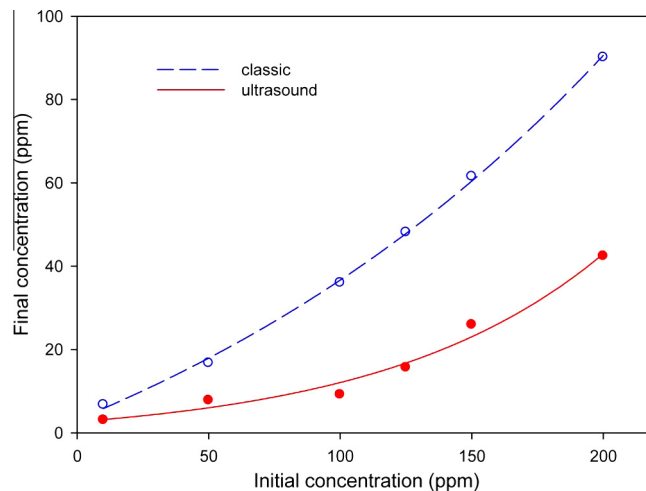


Fig. 7. Effect of initial concentration of 4-CP on its degradation (temp., 20 °C; time, 10 min; catalyst dosage, 0.07 g).

degradation rate was more effective in the presence of ultrasound. This is due to the increase of diffusion process and the number of new catalytic sites by the micro-jet and streaming effects of the cavitation process. According to Fig. 6, the proper amount of catalyst for this removal was about 0.07 g.

3.1.3. The initial concentration

The effect of pollutant concentration on its degradation was investigated in the range of 10–200 mg L⁻¹. Fig. 7 shows that by increasing the initial concentration, the final concentration remaining in the solution was also increased. This should be explained based on the constant catalytic available sites for the constant amount of the catalyst. In addition, the final concentration remaining in the solution under ultrasound was much lower than conventional method. This might be due to the cavitation process that leads to an enhancement of the reaction rate of active species

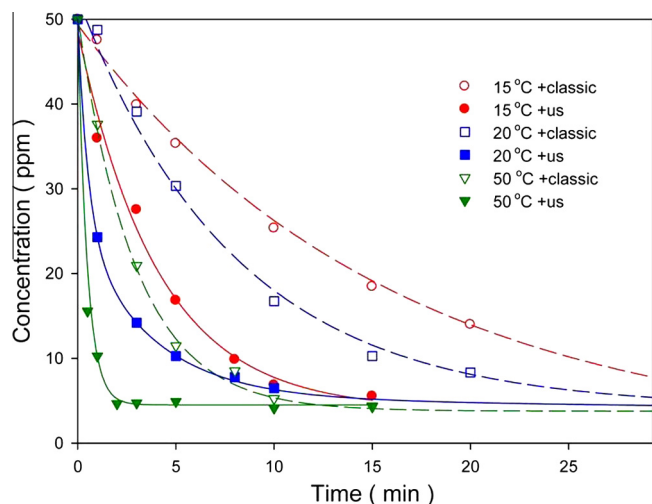


Fig. 8. Effect of temperature on the degradation of 4-CP with time (stirring speed 400 rpm; initial concentration of 4-CP 50 mg L⁻¹; catalyst dosage, 0.07 g; pH, 2.5).

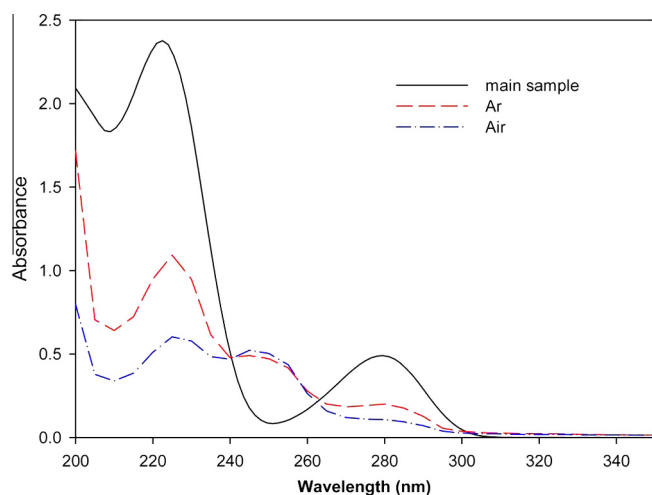


Fig. 9. Effect of gas atmosphere on the catalytic activity of LSMO nanoparticles (stirring speed, 400 rpm; initial concentration, 50 mg L⁻¹; catalyst dosage, 0.07 g; time, 10 min; pH, 2.5).

Table 1

Kinetic rate constants in the presence and absence of ultrasound at different temperatures.

<i>t</i> (°C)	Classic method		Sonicated method	
	<i>k</i> ₂ (L mg ⁻¹ min ⁻¹)	<i>R</i> ²	<i>k</i> ₂ (L mg ⁻¹ min ⁻¹)	<i>R</i> ²
15	0.0025	0.98	0.0098	0.99
20	0.0052	0.99	0.0133	0.99
30	0.0089	0.98	0.0205	0.99
50	0.0127	0.98	0.0923	0.99

with pollutant and applied other affects such as cleaning and sweeping of nanoparticle surface by acoustic micro-streaming which allows more active sites to be available.

3.1.4. The temperature of medium

The effect of temperature was investigated in the range of 15–50 °C for the catalytic degradation of 4-CP. Fig. 8 shows the concentration of 4-CP versus reaction time at different temperatures. The increase of temperature significantly enhanced the degradation. A

Table 2

Reusability of LSMO catalyst.

Catalyst	Percent of degradation	
	Classic method	Sonicated method
La _{0.7} Sr _{0.3} MnO ₃	73.51 ± 1.36	90.54 ± 0.18
Reused-1cycle	73.00 ± 0.31	91.24 ± 0.18
Reused-2cycle	72.41 ± 1.56	90.89 ± 1.07
Reused-3cycle	69.75 ± 0.99	91.33 ± 0.12
Reused-4cycle	65.47 ± 0.83	90.51 ± 0.21

removal of 90% and 54% of 4-CP was obtained after 3 min at 50 °C in the presence and absence of ultrasound, respectively. However, a lower catalytic performance was observed at lower temperatures, which might be related to the diffusion process of the species. In addition, a higher degradation of intermediate was obtained after 45 min at 80 °C in the presence of ultrasound (Fig. 3).

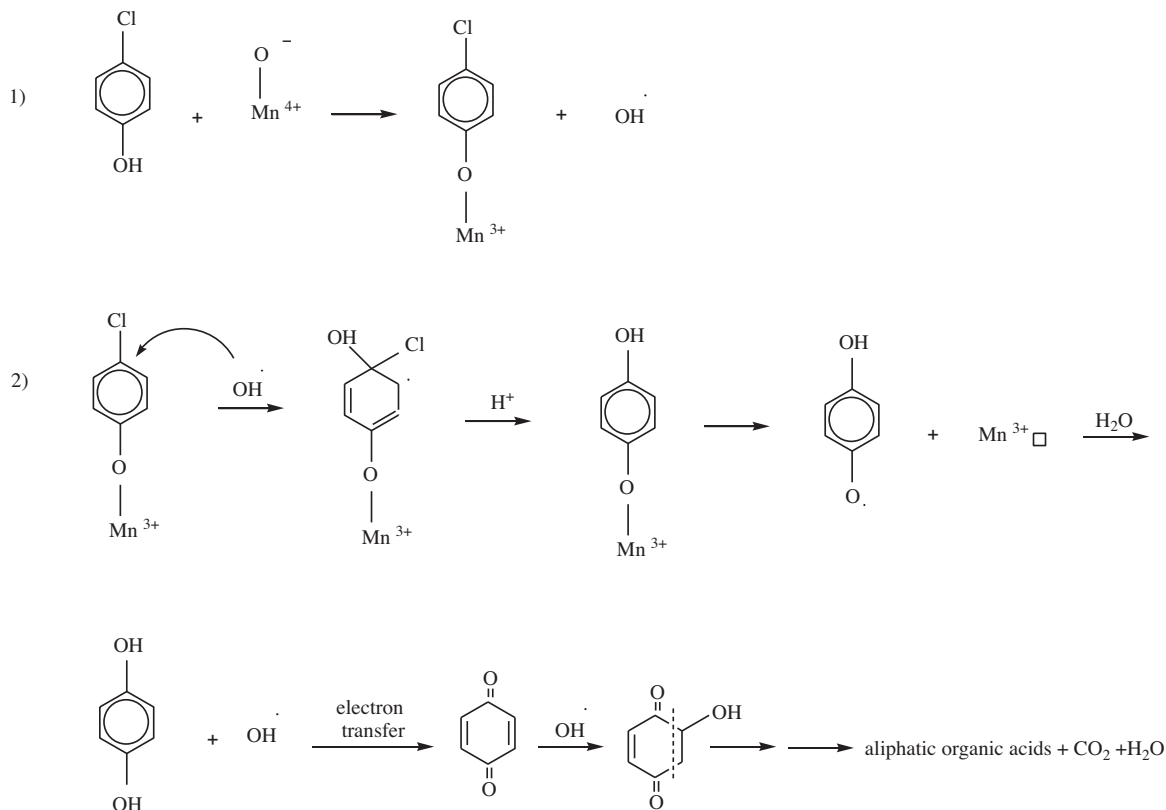
For both methods, by increasing the temperature, the rate of degradation was enhanced. The rate was higher in the presence of ultrasound than its absence. These behaviors are in agreement with the other reports [48–53]. However, the results obtained for decomposition with increasing temperature are in disagreement with that expected ultrasound is less effective at higher temperatures. This is due to an increase of vapor pressure of water that leads to cushion the collapse and the lower production of radicals [54,55]. Nevertheless, in this system, the presence of the catalyst as a solid particle can extremely alters the situation. In addition, the experimental results in the presence and absence of ultrasound confirmed that the catalyst alone play a critical role in the degradation. It seems that ultrasound facilitates the catalytic effects on the degradation of the pollutant. Based on Fig. 3, the sonication of the solution without catalyst for one hour had a negligible effect. This observation was also confirmed the basic role of the catalyst in degradation.

3.2. Mechanism of degradation

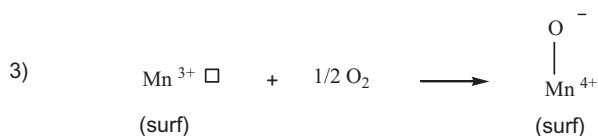
Oxidation reaction on perovskite catalysts are often described by the Mars van Krevelen model [56] (Fig. 7S in supporting). A two step reaction was proposed which involves the reaction between the oxidable reactant and the active oxygen on the surface, and then re-oxidation of the reduced catalyst site by the gas phase oxygen. Based on this model, the adsorption of molecular oxygen on the surface is assumed to be the rate limiting step of the overall reaction. For confirming the role of oxygen in this process, the catalytic degradation was carried out under Ar atmosphere in conventional method. According to Fig. 9, the catalytic activity of LSMO decreases in the presence of argon gas. This means that the ambient oxygen is effective on the catalytic activity of LSMO nanoparticles which is in agreement with Mars-van Krevelen mechanism. In addition, in Ar atmosphere, the activity of the nanocatalyst was not stopped and the activity in the absence of oxygen (Ar atmosphere) was lower than that in the presence of gas phase oxygen. These behaviors could be explained that when the degradation is carried out in the absence of oxygen, the lattice oxygen may be involved in the process, whereas, in the presence of oxygen, both adsorbed oxygen and lattice oxygen can be involved.

The following mechanism can be in agreement with previous results obtained by S. Kaliaguine and et al. [57–61]. Based on these studies, the reactive oxygen located on Mn⁴⁺ valency sites may be considered as any of the surface oxygen species (O₂⁻, O⁻ and/or O²⁻) in the 4-CP oxidation process. The reaction of reactive oxygen with the 4-CP molecules leads to the formation of Mn³⁺ reduced sites that can be reoxidized by adsorption of a dissolved O₂ mole-

cule for the regeneration of active sites. In fact, it is necessary an anion vacancy and a $\text{Mn}^{n+} \text{O}^-$ site produced after the calcination step [60]. In according to the mechanism proposed, the oxidation reaction starts with adsorption of 4-CP on the catalyst surface and simultaneous tearing off of an H-atom from the phenolic OH-group. This process combines with the active oxygen (O^-) of the catalyst to form surface OH^\cdot that participate further in the next steps of the surface oxidation and the reduced sites (reactions 1 and 2) (where \square is an anion vacancy)



The reduced sites ($\text{Mn}_{(\text{surf})}^{3+}$) can be re-oxidized by adsorption of a dissolved O_2 molecule for active site regeneration (reaction 3). In addition, the low amount of TOC determines the most products must be gaseous because of they do not stay in the solution



3.3. Kinetics of degradation

Fig. 8S(a, b) in supporting shows the rate of catalytic decomposition of 4-CP under the applied conditions for both methods. It confirms that the degradation is second-order for both methods by the linearity of the plots of $1/C$ versus contact time at different temperatures.

Table 1 indicates the rate constants (k) for the degradation of 4-CP at different temperatures. In both methods by increasing the temperature, the rate constant of degradation increases. The rate constants are more in the presence of ultrasound than in the ab-

sence of ultrasound which is due to the chemical and mechanical effects of ultrasound.

3.4. Reusability of the catalyst

Table 2 shows the percent of degradation by the recoverable magnetic nanocatalyst under ultrasound and conventional methods in the several successive cycles. All experiments were conducted with 0.07 g nanocatalyst at 20°C for 10 min. The catalyst

was separated by magnet and after drying by air it was used repeatedly in direct addition to the solution. The results indicated that the catalyst can be used successfully up to five consecutive cycles without changing and significant loss in activity especially for the sample under sonication. In addition, the nanocatalyst can be used successively without need to recalcination in contrast to the other works [21,22]. The high reusability in the sono-assisted reaction as compared with the classic method (where a gradual decrease of the degradation is observed (Table 2)) is due to the self-cleaning and removal of surface contamination of the catalyst surface by the action of the ultrasound [16,62,63].

4. Conclusion

The removal of 4-CP has been investigated under different experimental conditions in the presence and absence of ultrasound. This study exploited the applicability of lanthanum strontium manganite for the catalytic degradation of 4-CP. The degradation has been studied at different temperatures, pH, catalyst dosage, and initial concentration of 4-CP for both methods. Decreasing in the concentration of 4-CP and TOC under ultrasound achieved in a shorter time than conventional method. This is due to the cavitation process which increased the mass transfer, the sur-

face area of the catalyst, and the new catalytic sites. The kinetics of degradation was second-order for both methods and more important the catalyst can be used up to five consecutive cycles with no significant loss in the activity and without need to recalcinate in contrast to the other works. Furthermore, the fast decrease of TOC and efficient use of this catalyst under mild condition for consecutive cycles makes this catalyst as an excellent candidate for the application in high level of wastewater treatment.

Acknowledgment

The authors would like to acknowledge Prof. Christian Rüssel, Prof. Christian Bocker and Mr. A. Keshavarzi for performing the TEM analysis at Otto-Schott-Institut, Jena University, Fraunhoferstr. 6, 07743 Jena, Germany. The support of Ferdowsi University of Mashhad (Research and Technology) for this work (code 3/16942, date 17/12/1389) is appreciated.

Appendix A. Supplementary data

Supplementary data associated with this article can be found, in the online version, at <http://dx.doi.org/10.1016/j.ultsonch.2013.03.009>.

References

- [1] Y. Du, M. Zhou, L. Lei, The role of oxygen in the degradation of p-chlorophenol by Fenton system, *J. Hazard. Mater.* 139 (2007) 108–115.
- [2] O. Hamdaoui, E. Naffrechoux, Sonochemical and photSonochemical degradation of 4-chlorophenol in aqueous media, *Ultrason. Sonochem.* 15 (2008) 981–987.
- [3] M.H. Entezari, A. Heshmati, A. Sarafraz-yazdi, A combination of ultrasound and inorganic catalyst: removal of 2-chlorophenol from aqueous solution, *Ultrason. Sonochem.* 12 (2005) 137–141.
- [4] M. Blanco, L. Pizzio, Influence of the thermal treatment on the physicochemical properties and photocatalytic degradation of 4-chlorophenol in aqueous solutions with tungstophosphoric acid modified mesoporous titania, *Appl. Catal. A Gen.* 405 (2011) 69–78.
- [5] T.L. Lai, J.Y. Liu, K.F. Yong, Y.Y. Shu, C.B. Wang, Evaluation of bias potential enhanced photocatalytic degradation of 4-chlorophenol with TiO₂ nanotube fabricated by anodic oxidation method, *Chem. Eng. J.* 146 (2009) 30–35.
- [6] L. Calvo, M.A. Gilarranz, J.A. Casas, A.F. Mohedano, J.J. Rodríguez, Ydrodechlorination of 4-chlorophenol in water with formic acid using a Pd/activated carbon catalyst, *J. Hazard. Mater.* 161 (2009) 842–847.
- [7] W. Bian, X. Song, D. Liu, J. Zhang, X. Chen, The intermediate products in the degradation of 4-chlorophenol by pulsed high voltage discharge in water, *J. Hazard. Mater.* 192 (2011) 1330–1339.
- [8] U.J. Gaya, A.H. Abdullah, Z. Zainal, M.Z. Hussein, Photocatalytic treatment of 4-chlorophenol in aqueous ZnO suspension: intermediates, influence of dosage and inorganic anions, *J. Hazard. Mater.* 168 (2009) 57–63.
- [9] S.G. Christoskova, M. Stoyanova, M. Georgieva, Low-temperature iron-modified cobalt oxide system Part 2. catalytic oxidation of phenol in aqueous phase, *Appl. Catal. A Gen.* 208 (2001) 243–249.
- [10] R. Kidak, N.H. Ince, Ultrasonic destruction of phenol and substituted phenols: a review of current research, *Ultrason. Sonochem.* 13 (2006) 195–199.
- [11] P.R. Gogate, Treatment of wastewater streams containing phenolic compounds using hybrid techniques based on cavitation: a review of the current status and the way forward, *Ultrason. Sonochem.* 15 (2008) 1–15.
- [12] R.J. Emery, M. Papadaki, D. Mantzavinos, Sonochemical degradation of phenolic pollutants in aqueous solutions, *Environ. Technol.* 24 (2003) 1491–1500.
- [13] D.J. Flannigan, K.S. Suslick, Plasma formation and temperature measurement during single-bubble cavitation, *Nature* 434 (2005) 52–55.
- [14] M.H. Entezari, M. Mostafai, A. Sarafraz-yazdi, A combination of ultrasound and a bio catalyst: removal of 2-chlorophenol from aqueous solution, *Ultrason. Sonochem.* 13 (2006) 37–41.
- [15] N. Ghows, M.H. Entezari, Exceptional catalytic efficiency in mineralization of the reactive textile azo dye (RB5) by a combination of ultrasound and core-shell nanoparticles (CdS/TiO₂), *J. Hazard. Mater.* 195 (2011) 132–138.
- [16] N. Ghows, M.H. Entezari, Kinetic investigation on sono-degradation of Reactive Black 5 with core-shell nanocrystal, *Ultrason. Sonochem.* 20 (2013) 386–394.
- [17] M.H. Entezari, C. Petrier, A combination of ultrasound and oxidative enzyme: sono- biodegradation of phenol, *Appl. Catal. B Environ.* 53 (2004) 257–263.
- [18] J.K. Kim, F. Martinez, I.S. Metcalfe, The beneficial role of use of ultrasound in heterogeneous Fenton-like system over supported copper catalysts for degradation of p-chlorophenol, *Catal. Today* 124 (2007) 224–231.
- [19] C. Resini, F. Catania, S. Berardinelli, O. Paladino, G. Busca, Catalytic wet oxidation of phenol over lanthanum strontium manganite, *Appl. Catal. B Environ.* 84 (2008) 678–683.
- [20] Y. Yang, Y. Sun, Y. Jiang, Structure and photocatalytic property of perovskite and perovskite-related compounds, *Mater. Chem. Phys.* 96 (2006) 234–239.
- [21] C. Singh, M. Rakesh, Oxidation of phenol using LaMnO₃ perovskite, TiO₂, H₂O₂ and UV radiation, *Indian J. Chem. Technol.* 17 (2010) 451–454.
- [22] J.L. Sotelo, G. Ovejero, F. Martinez, J.A. Melero, A. Milieni, Catalytic wet peroxide oxidation of phenolic solutions over a LaTi_{1-x}Cu_xO₃ perovskite catalyst, *Appl. Catal. B Environ.* 47 (2004) 281–294.
- [23] S.J. Singh, R.V. Jayaram, Oxidation of alkylaromatics to benzylic ketones using TBHP as oxidant over LaMO₃ (M = Cr, Co, Fe, Mn, Ni) perovskites, *Catal. Commun.* 10 (2009) 2004–2007.
- [24] S. Daengsakul, C. Thomas, I. Thomas, C. Mongkolkachit, S. Siri, V. Amornkitbamrung, S. Maensiri, Magnetic and cytotoxicity properties of La_{1-x}Sr_xMnO₃ (0 ≤ x ≤ 0.5) nanoparticles prepared by a simple thermal hydro-decomposition, *Nanoscale Res. Lett.* 4 (2009) 839–845.
- [25] S. Daengsakul, C. Mongkolkachit, C. Thomas, S. Siri, I. Thomas, V. Amornkitbamrung, S. Maensiri, A simple thermal decomposition synthesis, magnetic properties, and cytotoxicity of La_{0.7}Sr_{0.3}MnO₃ nanoparticles, *Appl. Phys. A Mater. Sci. Process.* 96 (2009) 691–699.
- [26] S.N. Kale, S. Arora, K.R. Bhayani, K.M. Paknikar, M. Jani, U.V. Wagh, S.D. Kulkarni, S.B. Ogale, Cerium doping and stoichiometry control for biomedical use of La_{0.7}Sr_{0.3}MnO₃ nanoparticles: microwave absorption and cytotoxicity study, *Nanomed. Nanotechnol. Biol. Med.* 2 (2006) 217–221.
- [27] E. Feng, Y. Zhou, F. Zhao, X. Chen, L. Zhang, H. Jiang, H. Liu, Gold-catalyzed tandem reaction in water: an efficient and convenient synthesis of fused polycyclic indoles, *Green Chem.* 14 (2012) 1888–1895.
- [28] P. Anastas, N. Eghbali, *Green chemistry: principles and practice*, Chem. Soc. Rev. 39 (2010) 301–312.
- [29] D.R. Sahu, B.K. Roul, P. Pramanik, J.L. Huang, Synthesis of La_{0.7}Sr_{0.3}MnO₃ materials by versatile chemical technique, *Phys. B Condens. Matter* 369 (2005) 209–214.
- [30] F. Chen, H.W. Liu, K.F. Wang, H. Yu, S. Dong, X.Y. Chen, X.P. Jiang, Z.F. Ren, J.M. Liu, Synthesis and characterization of La_{0.82}Sr_{0.175}MnO₃ nanowires, *J. Phys. Condens. Matter* 17 (2005) L467–L475.
- [31] T. Zhang, C.G. Jin, T. Qian, X.L. Lu, J.M. Bai, X.G. Li, Hydrothermal synthesis of single-crystalline La_{0.5}Ca_{0.5}MnO₃ nanowires at low temperature, *J. Mater. Chem. B* 14 (2004) 2787–2789.
- [32] D. Zhu, H. Zhu, Y.H. Zhang, Hydrothermal synthesis of single-crystal La_{0.5}Sr_{0.5}MnO₃ nanowire under mild conditions, *J. Phys. Condens. Matter.* 14 (2002) L519–L524.
- [33] D. Zhu, H. Zhu, Y. Zhang, Hydrothermal synthesis of La_{0.5}Ba_{0.5}MnO₃ nanowires, *Appl. Phys. Lett.* 80 (2002) 1634–1636.
- [34] R.F.C. Marques, M. Jafelici, C.O. Paiva-Santos, R.F. Jardim, J.A. Souza, L.C. Varanda, R.H.M. Godoi, Nanoparticle synthesis of La_{1-x}Sr_xMnO₃ (0.1, 0.2 and 0.3) perovskites, *IEEE Trans. Magn.* 38 (2002) 2892–2894.
- [35] G. Pang, X. Xu, V. Markovich, S. Avivi, O. Palchik, Y. Koltypin, G. Gorodetsky, Y. Yeshurun, H. Peter Buchkremer, A. Gedanken, Preparation of La_{0.7}Sr_{0.3}MnO₃ nanoparticles by sonication-assisted coprecipitation, *Mater. Res. Bull.* 38 (2003) 11–16.
- [36] N.A. Dhas, K.S. Suslick, Sonochemical preparation of hollow nanospheres and hollow nanocrystals, *J. Am. Chem. Soc.* 127 (2005) 2368–2369.
- [37] S. Anandan, F. Grieser, M. Ashokkumar, Sonochemical synthesis of Au–Ag core-shell bimetallic nanoparticles, *J. Phys. Chem. C* 112 (2008) 15102–15105.
- [38] A. Tieh, S. Krabnitzer, Y. Koltypin, A. Gedanken, Chloroethene dehalogenation with ultrasonically produced air-stable nano iron, *Ultrason. Sonochem.* 16 (2009) 617–621.
- [39] N. Ghows, M.H. Entezari, Ultrasound with low intensity assisted the synthesis of nanocrystalline TiO₂ without calcinations, *Ultrason. Sonochem.* 17 (2010) 878–883.
- [40] N. Ghows, M.H. Entezari, A novel method for the synthesis of CdS nanoparticles without surfactant, *Ultrason. Sonochem.* 18 (2011) 269–275.
- [41] N. Ghows, M.H. Entezari, Sono-synthesis of core-shell nanocrystal (CdS/TiO₂) without Surfactant, *Ultrason. Sonochem.* 19 (2012) 1070–1078.
- [42] N. Ghows, M.H. Entezari, Fast and easy synthesis of core-shell nanocrystal (CdS/TiO₂) at low temperature by micro-emulsion under ultrasound, *Ultrason. Sonochem.* 18 (2011) 629–634.
- [43] A.A. Rabelo, M. Cardoso de Macedo, D. Maria de Araujo Melo, C.A. Paskocimas, A.E. Martinelle, R. Maribondo do Nascimento, Synthesis and characterization of La_{1-x}Sr_xMnO₃ powders obtained by the polymeric precursor route, *Mater. Res.* 14 (2011) 91–96.
- [44] R. Vargas, C. Borras, J. Mostany, B.R. Scharifker, Measurement of phenols deaomatization via electrolysis, *Water Res.* 44 (2010) 911–917.
- [45] M. Kubo, K. Matsuoka, A. Takahashi, N. Shibasaki-Kitakawa, T. Yonemoto, Kinetics of ultrasonic degradation of phenol in the presence of TiO₂ particles, *Ultrason. Sonochem.* 12 (2005) 263.
- [46] A. Keck, E. Gilbert, R. Köster, Influence of particles on sonochemical reactions in aqueous solutions, *Ultrasonics* 40 (2002) 661–665.
- [47] T. Tuziuti, K. Yasui, M. Sivakumar, Y. Iida, Correlation between acoustic cavitation noise and yield enhancement of sonochemical reaction by particle addition, *J. Phys. Chem. A* 109 (2005) 4869–4872.
- [48] M.A. Behnajady, N. Modirshahla, M. Shokri, B. Vahid, Effect of operational parameters on degradation of Malachite Green by ultrasonic irradiation, *Ultrason. Sonochem.* 15 (2008) 1009–1014.

- [49] M.H. Priya, Giridhar Madras, Kinetics of TiO₂-catalyzed ultrasonic degradation of Rhodamine dyes, *Ind. Eng. Chem. Res.* 45 (2006) 913–921.
- [50] J. Wang, B. Guo, X. Zhang, Z. Zhang, J. Han, J. Wu, Sonocatalytic degradation of methyl orange in the presence of TiO₂ catalysts and catalytic activity comparison of rutile and anatase, *Ultrason. Sonochem.* 12 (2005) 331–337.
- [51] M. Li, J.-T. Li, H.-W. Sun, Decolorizing of azo dye Reactive red 24 aqueous solution using exfoliated graphite and H₂O₂ under ultrasound irradiation, *Ultrason. Sonochem.* 15 (2008) 717–723.
- [52] H. Ghodbane, O. Hamdaoui, Degradation of Acid Blue 25 in aqueous media using 1700 kHz ultrasonic irradiation: ultrasound/Fe(II) and ultrasound/H₂O₂ combinations, *Ultrason. Sonochem.* 16 (2009) 593–598.
- [53] E.V. Rokhina, E. Repo, J. Virkutyte, Comparative kinetic analysis of silent and ultrasound-assisted catalytic wet peroxide oxidation of phenol, *Ultrason. Sonochem.* 17 (2010) 541–546.
- [54] Y. Jiang, C. Petrier, T.D. Waite, Sonolysis of 4-chlorophenol in aqueous solution: effects of substrate concentration, aqueous temperature and ultrasonic frequency, *Ultrason. Sonochem.* 13 (2006) 415–422.
- [55] T.J. Mason, J.P. Lorimer, *Sonochemistry: Theory Applications and Uses of Ultrasound in Chemistry*, Ellis Horwood, Chichester, UK, 1998.
- [56] R.J. Bell, G.J. Millar, J. Drennan, Influence of synthesis route on the catalytic properties of La_{1-x}Sr_xMnO₃, *Solid State Ionics* 131 (2000) 211–220.
- [57] S. Kaliaguine, A. Van Neste, V. Szabo, J.E. Gallot, M. Bassir, R. Muzychuk, Perovskite-type oxides synthesized by reactive grinding: Part I. Preparation and characterization, *Appl. Catal. A* 209 (2001) 345.
- [58] S. Royer, F. Bérubé, S. Kaliaguine, Effect of the synthesis conditions on the redox and catalytic properties in oxidation reactions of LaCo_{1-x}Fe_xO₃, *Appl. Catal. A* 282 (2005) 273–284.
- [59] R. Zhang, A. Villanueva, H. Alamdari, S. Kaliaguine, SCR of NO by propene over nanoscale LaMn_{1-x}Cu_xO₃ perovskites, *Appl. Catal. A* 307 (2006) 85.
- [60] B. Levasseur, S. Kaliaguine, Methanol oxidation on LaBO₃ (B = Co, Mn, Fe) perovskite-type catalysts prepared by reactive grinding, *Appl. Catal. A General* 343 (2008) 29–38.
- [61] S. Royer, D. Duprez, S. Kaliaguine, Role of bulk and grain boundary oxygen mobility in the catalytic oxidation activity of LaCo_{1-x}Fe_xO₃, *J. Catal.* 234 (2005) 364–375.
- [62] D.E. Kritikos, N.P. Xekoukoulotakis, E. Psillakis, D. Mantzavinos, Photocatalytic degradation of reactive black 5 in aqueous solutions: Effect of operating conditions and coupling with ultrasound irradiation, *Water Res.* 41 (2007) 2236–2246.
- [63] N. Arul Dhas, K.S. Suslick, Sonochemical preparation of hollow nanospheres and hollow nanocrystals, *J. Am. Chem. Soc.* 127 (2005) 2368–2369.